Am J Cancer Res 2014;4(6):683-697
www.ajcr.us /ISSN:2156-6976/ajcr0002285

Original Article

SPRY1 promotes the degradation of uPAR and inhibits uPAR-mediated cell adhesion and proliferation

Xiufeng Liu[1], Yan Lan[1], Di Zhang[1], Kai Wang[1], Yao Wang[1,3], Zi-Chun Hua[1,2]

[1]The State Key Laboratory of Pharmaceutical Biotechnology, College of Life Science, Nanjing University, 22 Han Kou Road, Nanjing 210093, P. R. China; [2]Changzhou High-Tech Research Institute of Nanjing University and Jiangsu TargetPharma Laboratories Inc., Changzhou 213164, P. R. China; [3]Division of Critical Care and Surgery, St. George Hospital, University of New South Wales, Sydney, NSW2217, Australia

Received September 3, 2014; Accepted October 18, 2014; Epub November 19, 2014; Published November 30, 2014

Abstract: Urokinase plasminogen activator receptor (uPAR) is a GPI anchored cell surface protein that is closely associated with invasion, migration, and metastasis of cancer cells. Many functional extracellular proteins and transmembrane receptors interact with uPAR. However, few studies have examined the association of uPAR with cytoplasm proteins. We previously used yeast two-hybrid screening to isolate several novel uPAR-interacting cytoplasmic proteins, including Sprouty1 (SPRY1), an inhibitor of the (Ras-mitogen-activated protein kinase) MAPK pathway. In this study, we show that SPRY1 interacts with uPAR and directs it toward lysosomal-mediated degradation. Overexpression of SPRY1 decreased the cell surface and cytoplasmic uPAR protein level. Moreover, SPRY1 overexpression augmented uPAR-induced cell adhesion to vitronectin as well as proliferation of cancer cells. Our results also further support the critical role of SPRY1 contribution to tumor growth. In a subcutaneous tumor model, overexpression of SPRY1 in HCT116 or A549 xenograft in athymic nude mice led to great suppression of tumor growth. These results show that SPRY1 may affect tumor cell function through direct interaction with uPAR and promote its lysosomal degradation.

Keywords: SPRY1, uPAR, degradation, adhesion, proliferation

Introduction

uPAR is a highly glycosylated cell surface protein that lacks transmembrane and intracellular domains and attaches to the plasma membrane by a glycosyl phosphatidylinositol (GPI) anchor. Elevated uPAR expression has been detected in many human cancers, including solid tumors, leukemias and lymphomas, and is associated with poor prognosis [1]. One of the most critical roles of uPAR is its involvement in the uPA-uPAR system to promote proteolysis of the extracellular matrix (ECM). uPAR-bound uPA subsequently converts plasminogen to active plasmin that facilitates the degradation of ECM and invasion of cancer cells. uPAR has also been implicated in several tumor processes through interactions with other cell surface molecules. Vitronectin is another ligand for uPAR [2], and uPAR associated with vitronectin can dramatically increase cell adhesion to vitronectin.

Many studies have shown that uPAR functions as a signaling receptor, interacting with other molecules, such as integrins, caveolin, G protein-coupled receptors and growth factor receptors [2-4], to relay its downstream signals. Signaling through uPAR activates the Tyr kinases focal adhesion kinase (FAK) and the MAPK pathway. For example, reduction of uPAR by uPAR shRNA resulted in reduced phosphor-FAK expression levels in pre-established medulloblastoma in nude mice [5]. Furthermore, knockdown of uPAR suppresses the phosphorylation of FAK, p38MAPK, JNK and ERK1/2 in glioma [6]. uPAR can be internalized to the cytoplasm through its interaction with low-density lipoprotein receptor-related protein (LRP-1) [7] or endocytic receptor 180 (ENDO180) [8, 9]. Recent studies revealed that uPAR can be constitutively internalized through a ligand-independent manner [10]. In addition, uPAR can also be recycled back from the endocytic compartment to the plasma membrane. The consti-

tutive internalization, recycling and degradation of uPAR are key events that determine the distribution of uPAR on the plasma membrane, thus controlling uPAR functions including proteolysis and non-proteolytic functions. Soluble uPAR (suPAR) is another form of uPAR that is released from the cell surface through the cleavage of GPI-anchored uPAR. Three different suPAR forms (suPARI-III, suPARII-III, and suPARI) have been detected in blood, urine and cerebrospinal fluid. Studies have shown that elevated suPAR is closely associated with some physiological and pathological events, including respiratory cancer, inflammation [11, 12], focal segmental glomerulosclerosis, type 2 diabetes and progressive liver fibrosis [13, 14]. Thus, increased plasma suPAR levels may serve as a useful diagnostic marker.

We previously used yeast two-hybrid screening to isolate several novel uPAR-interacting cytoplasmic proteins, including SPRY1. SPRY1 is an inhibitor of the MAPK pathway, was first identified in Drosophila as an inhibitor of FGF receptor signaling during tracheal development. However, the stage at which SPRY blocks MAPK activation remains controversial [15]. SPRY proteins can interact with multiple components of the Ras/MAPK pathway, including Grb2, FRS2, Shp2, c-Cbl, Raf1 and GAP1 [16-20]. In mammals, four SPRY genes (SPRY1–4) have been found. SPRY1 has been proposed to function as a tumor suppressor gene in various tumor types. Several cancer cells show a low basal expression of SPRY1, such as breast, prostate and liver cancers [21-23]. A recent study showed that SPRY1 is also a target of tumor suppressors, such as WT1 [24], angiostatic agent 16K prolactin and miR-21. Here we identified a previously unknown mechanism in which SPRY1 interacts with uPAR to promote its degradation by the lysosomal pathway. We investigated the possibility of SPRY1 function in adhesion and proliferation of cells.

Materials and methods

Reagents

Anti-uPAR (FL-290) rabbit polyclonal antibody was purchased from Santa Cruz Biotechnology (Dallas, TX). Antibody against SPRY1 was purchased from Abnova (Taipei City, Taiwan). Anti-phospho-ERK and anti-ERK antibodies were purchased from Cell Signaling Technology (Beverly, MA). Anti-tubulin antibody was purchased from Stratagene (La Jolla, CA). Antibodies against FAK and phospho-FAK (pY397) were purchased from BD Biosciences (San Diego, CA). Lipofectamine 2000 and Trizol were purchased from Invitrogen (Carlsbad, CA). The 2×SYBR Green QPCR Master Mix was purchased from Bio-RAD (Hercules, CA). E-64, MG132, protein inhibitor cocktail and cycloheximide (CHX) were obtained from Sigma (St Louis, MO).

Cell lines and transfection

HCT116 cells that stably express antisense uPAR cDNA fragment (antisense uPAR), control cells (Mock), HEK293 cells, and HEK293 cells stably transfected with uPAR (293-uPAR) were originally constructed in Dr. Yao Wang's lab (University of New South Wales, Sydney, Australia). HeLa, MCF-7, Caco2, A549, SW-620 and HCT116 cell lines were obtained from ATCC. All cells were cultured in DMEM or 1640 medium containing 10% FBS, l-glutamine (300 μg/ml), penicillin (100 IU/ml) and streptomycin (100 μg/ml). Cells were seeded at 3×10^5 cells per well in 6-well plates and transfected with plasmid in antibiotic-free medium using Lipofectamine 2000, according to the manufacturer's instructions.

Constructs

Full-length wild-type hSPRY1 or uPAR were cloned into pRK5 vector (Flag-tagged, His-tagged, or untagged), and the resultant vectors were named pRK5-SPRY1, pRK5-SPRY1-Flag, pRK5-uPAR-His, and pRK5-uPAR.

Immunoblotting

Cells were lysed in lysis buffer (50 mM Tris-HCl, pH 7.4, 250 mM NaCl, 0.5% Triton-X 100, 50 mM NaF, 2 mM EDTA, 1 mM Na_3VO_4 and protein inhibitor cocktail) for 30 min and then centrifuged at 13,000 *g* for 15 min at 4°C. Protein concentration was assessed by Bradford protein assay. Protein samples (60 μg) were separated by SDS-PAGE and transferred to PVDF membranes. Membranes were subsequently blocked for 1 h at room temperature and further incubated at 4°C overnight with primary antibodies. Membranes were then incubated with secondary HRP-conjugated mouse or rabbit antibodies. Protein band intensities were quantified using the Image J software.

Immunofluorescence assay

Cells transfected with plasmids were grown on cover slips in 6-well plates, and 48 h post-transfection, the cells were fixed with 4% formaldehyde and permeabilized using 0.5% Triton-100. Cells were blocked with 3% BSA and then incubated with primary antibodies diluted in 3% BSA followed by incubation with secondary antibodies. Fluorescence images were obtained using a microscope (Carl Zeiss, Oberkochen, Germany).

Adhesion assays

For adhesion assays, 48-well plates were coated with 10 μg/ml vitronectin, fibronectin or 1% BSA in PBS (uncoated plastic), and incubated overnight at 4°C. The plates were then blocked for 1 h at room temperature with 1% BSA in PBS. Cells were transfected with pRK5-SPRY1 or pRK5 empty plasmids. After 24 h, cells were harvested and washed three times in PBS, and 1×10^5 cells were plated in each coated well and incubated for 1 h at 37°C. Attached cells were fixed with 4% paraformaldehyde in PBS for 10 min and then incubated with 2% methanol for 10 min. The cells were stained with 0.5% crystal violet in 20% methanol. Images were captured using the 10x objective lens. To quantify the numbers of adherent cells, stain was eluted by 0.1 M sodium citrate in 50% ethanol, pH 4.2, and the absorbance at 595 nm was measured in a spectrophotometer.

Proliferation assays

Cells were transfected, and 24 h later, cells were plated in 48-well culture plates at a density of 1×10^4 cells per well in 10% FBS/DMEM. Proliferation was analyzed at different time points using MTT assay. Twenty μl of dimethyl thiazolyl diphenyl was added and the incubation continued for 4-6 h. Medium was removed, and 100 μl dimethyl sulfoxide (DMSO) was added to each well to dissolve the formazan by pipetting up and down several times. The absorbance, with a test wavelength of 570 nm and a reference wavelength of 630 nm, was measured. Empty wells (DMSO alone) were used as blanks. For continuous monitoring of changes in cell growth, approximately 1×10^4 cells/well were seeded onto E-plates and incubated for 30 min at room temperature, after which E-plates were placed onto the Real-Time Cell Analyzer (RTCA) station (xCELLigence System, Roche, Mannheim, Germany). Measurement of cell impedance was performed every half hour and continuously over 96 h.

Flow cytometry assays

Cell-surface uPAR levels were measured according to previously described methods [27]. Cells were harvested in PBS containing 5 mM EDTA and washed in PBS containing Ca^{2+} and Mg^{2+}, and then 5×10^5 cells were incubated with 10 μg/ml of rabbit anti-uPAR for 1 h at 4°C. Purified immunoglobulin was used as a negative control. The cells were then washed and incubated with a fluorescein isothiocyanate-labeled goat anti-rabbit IgG for 30 min at 4°C, then the cells were washed and analyzed by flow cytometry using a FACScan (Becton Dickinson, San Jose, CA).

Quantitative PCR

Cells were transfected with indicated plasmids. After 48 h, cells were washed with PBS, and then total RNA was isolated using TRIzol according to the manufacturer's instructions. Total RNA (1 μg) was reverse-transcribed using the PrimeScript RT reagent kit (TakaraBio, Tokyo, Japan), and 1 μl of a 1:10 dilution of the reverse transcription reaction was analyzed by real time quantitative PCR with a BioRad IQ5 system, using IQTMSYBR Green Supermix for qPCR kit. The mRNAs measured were normalized to β-actin mRNA. The relative level of expression was calculated with the formula $2^{-\Delta\Delta Ct}$. Primers used for PCR were as follows: uPAR F: 5'-AGCACGGCATCGTCA CCAACT-3'; uPAR R: 5'-TGGCTGGGGTGTTGAAGGTCT-3'; SPRY1 F: 5'-GCCTTCTTTGGATAGCCGTCAG-3'; SPRY1 R: 5'-TCATTGCTGCCTCTTATGGCC-3'; β-actin F: 5'-AGCACGGCATCGTCACCAACT-3'; β-actin R: 5'-TGGCTGGGGTGTTGAAGGTCT-3'.

Xenograft experiments

BALB/$_c$ female athymic nude mice (4-6 weeks) were purchased from the Laboratory Animal Center, Beijing, China, and housed in SPF and environmentally controlled conditions (22°C; a 12 h/12 h light/dark cycle, with the light cycle from 6:00 to 18:00 and the dark cycle from 18:00 to 6:00) and provided with pathogen-free food and water. The study protocol was approved by the local institution review boards

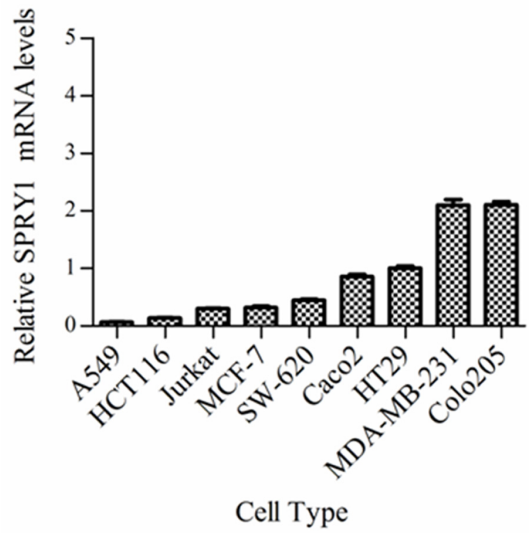

Figure 1. Real-time PCR results measuring relative levels of SPRY1 mRNA in the different cell types. Relative SPRY1 mRNA levels in different cell types were determined in relation to the housekeeping gene β-actin. mRNA levels obtained from HT29 cells were set at 1. All other levels were normalized to this value. Data from RT-PCR experiments are shown as means ± SEM of three independent experiments.

and animal study was carried out in accordance the established ethical guidelines for animal use and care at Nanjing University. Mice were inoculated subcutaneously on the mid-right flank with 5×10^5 cells in 100 μl PBS. About 1 week after injection of tumor cells, when tumors reached a size of approximately 150 mm^3, the mice were randomized into three groups (8 mice per group). The mice received direct local injections of the GenEscort™ Reagent (Wisegen Biotechnology, Nanjing, China) and plasmid complexes (5 ug plasmid per mouse). Injections were repeated every 3 days for a total of three times. Tumor volumes were measured using the formula: tumor volume (V) = length × $width^2$ × 0.5. Tumor doubling time refers to the time for a tumor to double in volume, and tumor growth delay time is the time interval to reach 1000 mm^3 compared with the PBS control group.

Statistical analysis

Paired Student's t test analysis was carried out on data using the SPSS software to assess statistical significance. Differences between experimental groups were considered significant when $p < 0.05$.

Results

Relative mRNA expression of SPRY1 in cancer cell lines

Figure 1 shows the relative quantifications of SPRY1 basal mRNA expression levels in different cancer cell lines. Lower basal levels of SPRY1 mRNA were detected in A549 and HCT116 cell lines, which have been considered high metastatic potential cell lines.

SPRY1 colocalizes with uPAR

Previous yeast two-hybrid and GST-pull down studies demonstrated a significant interaction between human SPRY1 and uPAR [28]. To determine intracellular localizations of both proteins, we performed immunofluorescence analysis of both endogenous and transfected uPAR and SPRY1 in HeLa cells. Immunofluorescence results showed co-localization of endogenous SPRY1 and uPAR within the cytoplasm (**Figure 2**, lower panel). SPRY1 showed low expression throughout the cytoplasm. The localizations of transfected SPRY1 and uPAR were consistent with endogenous results (**Figure 2**, middle and lower panels), with both proteins localized predominantly in the cytoplasm. These results provided further evidence to support the interaction between SPRY1 and uPAR *in vivo*.

SPRY1 promotes the lysosomal-mediated degradation of uPAR

Considering the opposite effect of SPRY1 and uPAR in regulating cancer progression, we investigated whether SPRY1 directly affects uPAR expression or vice versa. Low SPRY1 basal level cell lines, HCT116, A549 and 293-uPAR cells were transiently transfected with SPRY1 over-expression plasmids or empty vector and validated by both western blot and real time RT-PCR assay. As shown in **Figure 3**, over-expression of SPRY1 led to declined uPAR protein expression in total cell lysates (**Figure 3A**), whereas uPAR mRNA levels were unchanged (**Figure 3B**). These data suggested that SPRY1 may be involved in translation or protein stabilization of uPAR. We further validated the above results, 293-uPAR cells were transfected with increasing doses of SPRY1 expression plasmids. As shown in **Figure 3C**, over-expression of SPRY1 led to a dose-dependent decline of

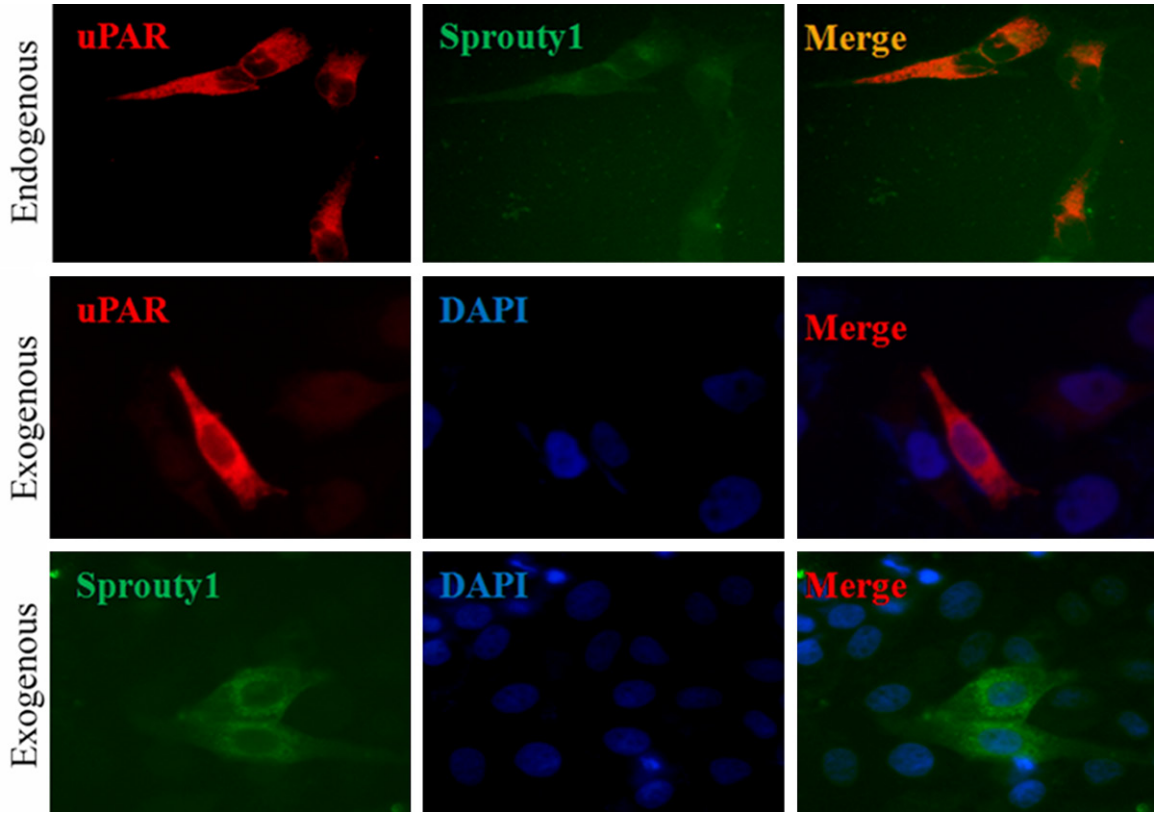

Figure 2. Immunofluorescence localization of SPRY1 and uPAR proteins in HeLa cells. Upper panel: Endogenous uPAR (red) and SPRY1 (green) co-localized in the cytoplasm. The cells were stained for SPRY1 using anti-SPRY1 antibody and Alexa Fluor 488-conjugated anti-mouse IgG (green). uPAR was detected by anti-uPAR antibody and Alexa Fluor 594-conjugated anti-rabbit IgG (red). Middle panel: Cells were transfected with pRK5-uPAR-His vector and exogenous uPAR was detected by immunostaining with anti-His antibody (in red). Lower panel: Cells were transfected with pRK5-SPRY1-Flag and exogenous SPRY1 was detected by immunostaining with anti-Flag antibody (in green). The nuclei were stained with DAPI (blue).

uPAR protein. Next, to eliminate the impact of the transfection reagents or procedure, we transfected equal amounts of empty vector (pRK5) or SPRY1 overexpression vector (pRK5-SPRY1). As shown in **Figure 3D**, empty vector transfection caused no alteration of uPAR protein level. In contrast, SPRY1 overexpression resulted in a dramatically decreased expression of uPAR protein.

There are two possible reasons for SPRY1-induced uPAR reduction: either inhibition of uPAR protein synthesis or alteration of uPAR protein degradation. As shown in **Figure 3E**, treatment with the protein synthesis inhibitor cycloheximide (CHX) did not inhibit SPRY1-induced uPAR reduction, suggesting that SPRY1 promoted the degradation of uPAR protein. To further evaluate degradation pathways possibly involved in the decrease of uPAR protein, 293-uPAR cells were transiently transfected with SPRY1 and incubated with the proteasome inhibitor MG132 (20 μM) or lysosomal inhibitor E-64 (20 μM) for indicated times. As shown in **Figure 3F**, E-64 treatment markedly blocked SPRY1-induced degradation of uPAR, but MG132 had no significant effect on the expression level of uPAR. This data suggests that SPRY1 enhances the degradation of uPAR mainly by the lysosomal pathway. Collectively, our results indicate that SPRY1 promotes uPAR degradation in a lysosomal pathway-dependent manner.

Effect of SPRY1 on cell adhesion

uPAR modulates several crucial cell behavior pathways, including adhesion, migration, invasion and proliferation. The above findings indicated SPRY1 promotes degradation of uPAR proteins, thus we next evaluated whether SPRY1 also affects uPAR-mediated cell behavior. First, we explored the functional consequence of SPRY1 up-regulation on uPAR-medi-

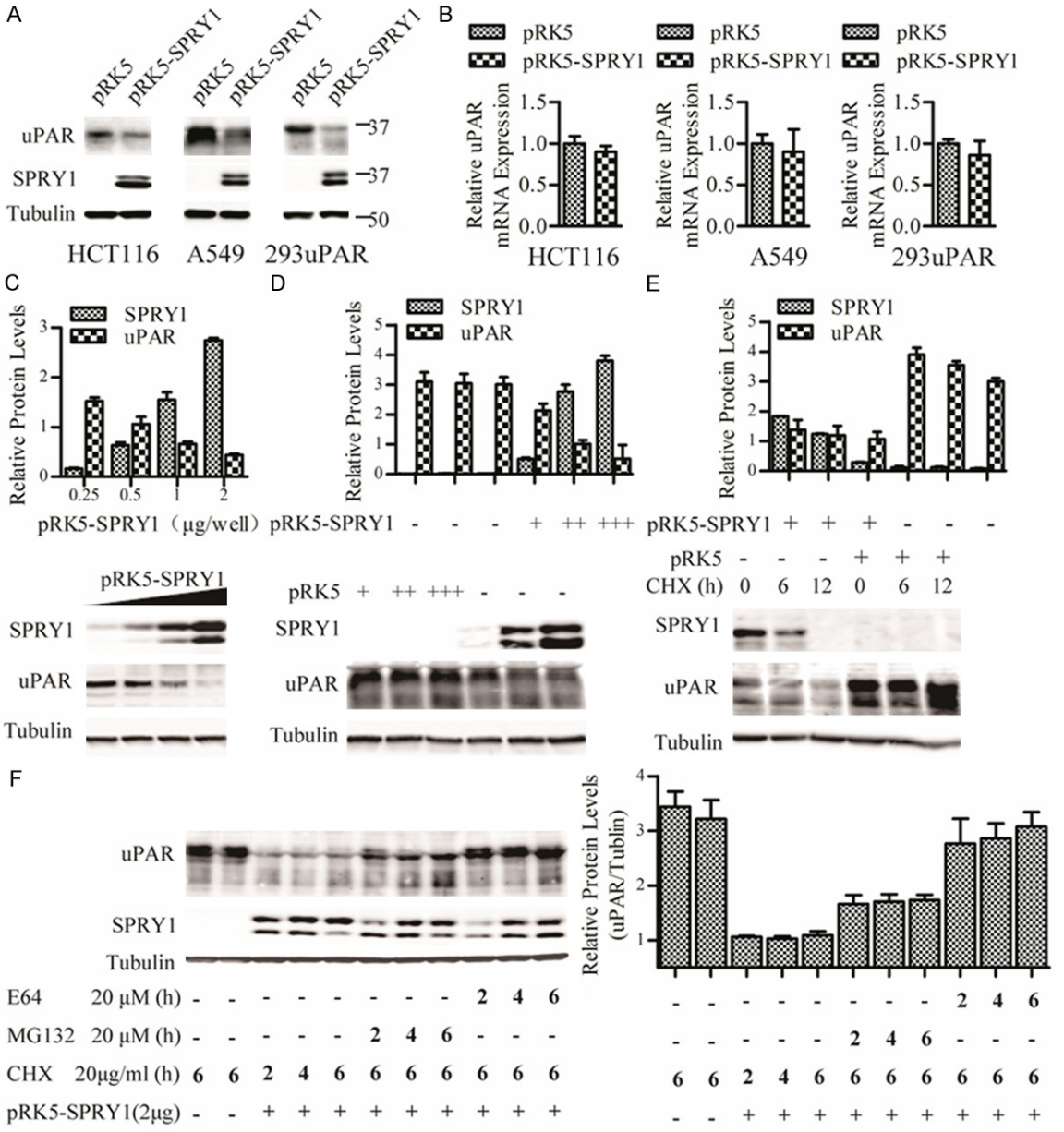

Figure 3. SPRY1 promotes uPAR downregulation. A. Western blot analysis of SPRY1 and uPAR protein amounts in total cell lysates from A549, HCT116 and 293-uPAR cells, transfected with pRK5-SPRY1 or pRK5. Tubulin was used as loading control. B. uPAR mRNA levels in A549, HCT116 and 293-uPAR cells (transfected with pRK5-SPRY1 or empty vector) were analyzed by quantitative PCR. β-actin was used for normalization of gene expression. C. Western blot analysis of SPRY1 and uPAR protein amounts in total cell lysates from 293-uPAR cells transfected with increasing amounts of SPRY1. Tubulin was used as loading control. D. Cells were transfected with increasing amounts of pRK5-SPRY1 or pRK5 empty vector, and cytotoxic effects of transfection to the expression of uPAR proteins were assessed. E. 293-uPAR cells transfected with pRK5-SPRY1 were treated with 20 μg/ml CHX and cells were lysed at the indicated times. Stability of uPAR was determined by western blot. Tubulin was used as loading control. F. SPRY1 decreases the stability of uPAR via the proteosome pathway. SPRY1 plasmids were transfected into 293-uPAR cells. Cells were treated with CHX (20 μg/ml), MG132 (20 μM) or E64 (20 μM) for indicated time points, and the cell lysates were evaluated by western blot. Each experiment was independently repeated three times. Tubulin was used as loading control. N.S.: no significant difference.

ated cell adhesion to vitronectin. As shown in **Figure 4A**, adhesion of HCT116 or A549 cells to vitronectin, but not to either fibronectin or BSA, was significantly decreased when cells were transfected with pRK5-SPRY1. Next, we investigated whether SPRY1-induced adhesion was dependent on uPAR. As shown in **Figure 4B**, 293 (uPAR-/-) cells showed weak adhesion to

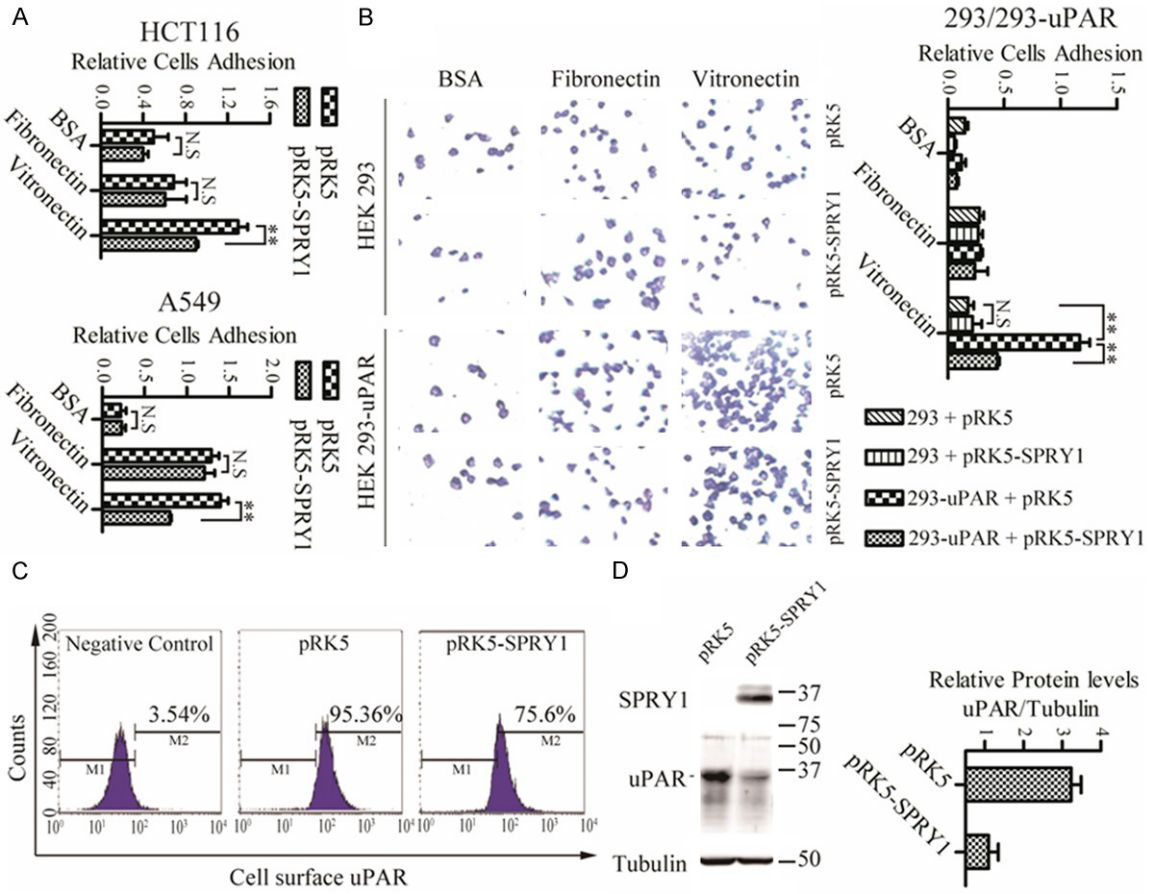

Figure 4. SPRY1 decrease of uPAR-mediated cell adhesion to vitronectin. (A) Fibronectin, vitronectin or BSA proteins were coated on the cell culture plate and blocked with BSA. HCT116 or A549 cells (transfected with pRK5-SPRY1 or empty vector) were spread on the immobilized proteins for 1 h. After washing, adherent cells were fixed with methanol, and stained with Giemsa stain. The relative numbers of cells were quantified using Safire Fluorescence Absorbance at OD550. The experiments were repeated twice and each column represents the mean of a triple determination. $**P < 0.01$: significantly different from the indicated control. (B) 293 and 293-uPAR cells were transfected with pRK5-SPRY1 or empty vector, and cell adhesion to fibronectin, vitronectin or BSA were evaluated as in HCT116 or A549 cells. Representative micrographs of the attached cells were examined microscopically. (C) 293-uPAR cells were transfected with pRK5-SPRY1 or empty vector, and 24 h later, the cell surface uPAR was analyzed by flow cytometry. (D) Whole cells in (C) were lysed by ultrasonic disruption and the expression of uPAR was detected by western blot. Tubulin was used as control. Each experiment was independently repeated three times. N.S.: no significant difference.

the vitronectin-coated substratum. However, in 293-uPAR cells transfected with uPAR vector, adhesion to the vitronectin-coated substratum was significantly increased. Meanwhile, overexpression of SPRY1 in 293-uPAR cells decreased the number of cells attached to vitronectin. However, overexpression of SPRY1 in 293 cells had no effect on adhesion to vitronectin.

Because uPAR-vitronectin interactions have been previously demonstrated, we inferred that increased SPRY1 expression may also decrease the amount of cell surface uPAR. To directly test this possibility, we analyzed cell surface uPAR in 293-uPAR cells by flow cytometric analysis. As shown in **Figure 4C**, when SPRY1 was overexpressed, cell surface uPAR was reduced by approximately 20%. The total amount of uPAR (in both the membrane and cytoplasmic fractions) was also detected by western blot. As shown in **Figure 4D**, total uPAR level was decreased by approximately 70%. Together this suggests that SPRY1 regulates cell adhesion through an uPAR-dependent mechanism.

Effect of SPRY1 on cell proliferation

To examine the effects of SPRY1 on cell proliferation, SPRY1 was overexpressed in HCT116 and A549 cells. We selected these cell lines

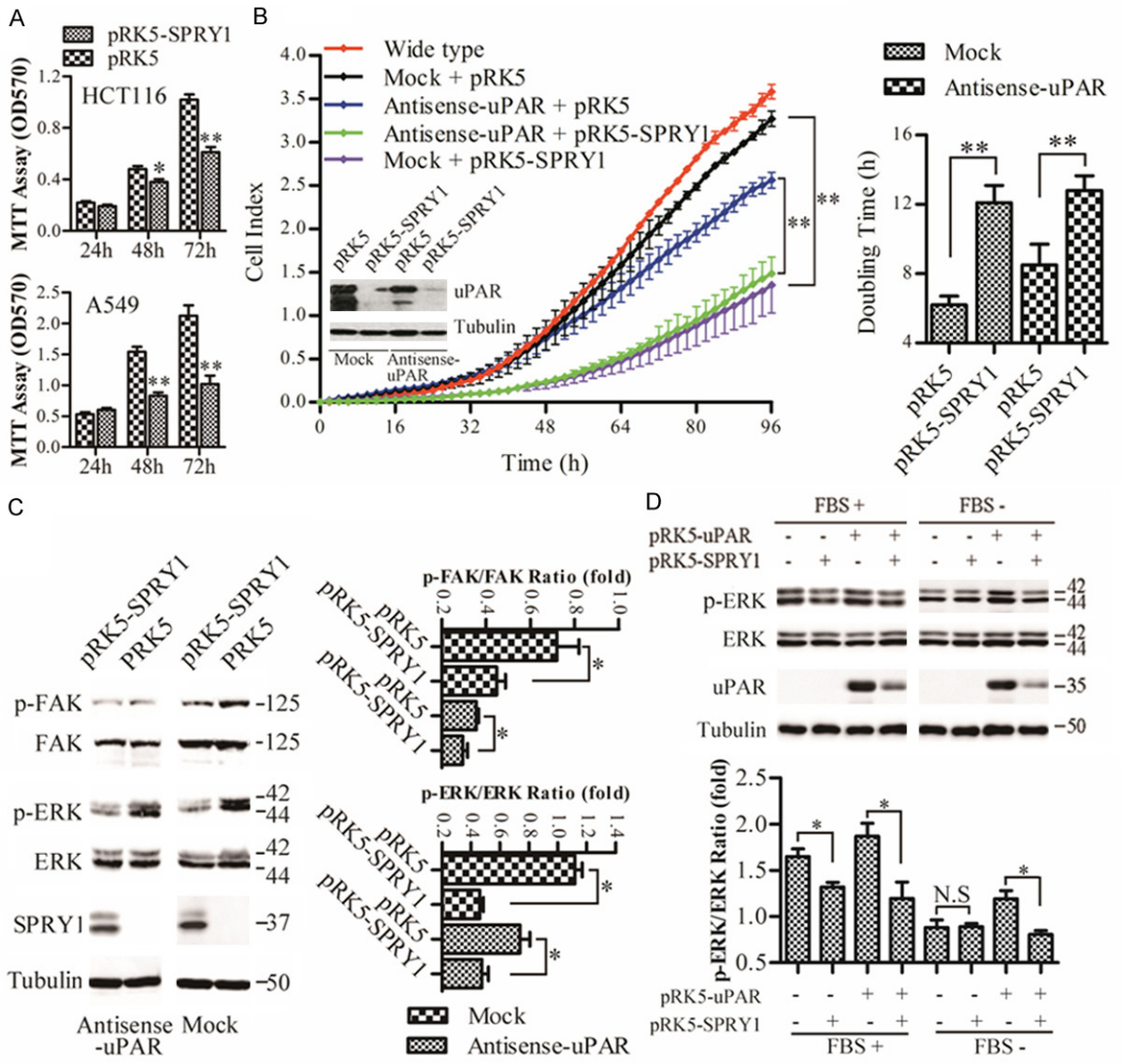

Figure 5. SPRY1 inhibition of uPAR induced cell proliferation. A. Effects of SPRY1 on the proliferation of HCT116 and A549 cells. Cells transfected with pRK5-SPRY1 or empty vector were seeded into 96-well plates. The cells were cultured for 24-72 h followed by MTT assay (OD570) to quantitate cell growth. Data are shown as mean ± SEM from three independent experiments. *$P < 0.05$, **$P < 0.01$ versus vector control. B. Effects of SPRY1 on the proliferation of antisense-uPAR or mock transfected HCT116 stable cell lines. Antisense-uPAR and mock cells were transfected with equal amounts of pRK5-SPRY1 or empty vector for 12 h, and then seeded on Real-Time Cellular Analysis (RTCA) 16 well E-plates with 1×10^4 cells/well (n = 3). Dynamic monitoring of cell proliferation was performed using the xCELLigence RTCA system for an additional 96 h. Relative cell doubling time from 0 to 48 h was performed using RTCA Software 1.2.1. The results are representative of two independent experiments performed in quadruplicate. *$P < 0.05$, **$P < 0.01$ versus indicated control. C. Effects of SPRY1 on the activation status of FAK and ERK in antisense-uPAR or mock cells. Cells were transiently transfected with pRK5-SPRY1 or empty vector for 48 h. ERK and FAK-397 phosphorylation was determined by western blot analysis. The intensities of the bands were quantified using ImageJ software. Data are from three independent experiments; *$P < 0.05$ versus indicated control. D. Effects of SPRY1 on uPAR-induced ERK activation. HCT116 cells were transfected with the indicated SPRY1 and uPAR expression vectors together or alone, and 36 h later, cells were continuously cultured in DMEM (without or with FBS added) for another 12 h. ERK phosphorylation was determined by western blot analysis. Data are from three independent experiments; *$P < 0.05$ versus indicated control.

because they have low basal expression of SPRY1 as detected by Q-PCR (**Figure 1**). Cells were transfected with SPRY1 or empty vector, and 24 h after transfection, cells were re-seeded and proliferation was analyzed at different time points (24, 48, 72 h) using MTT assay. As

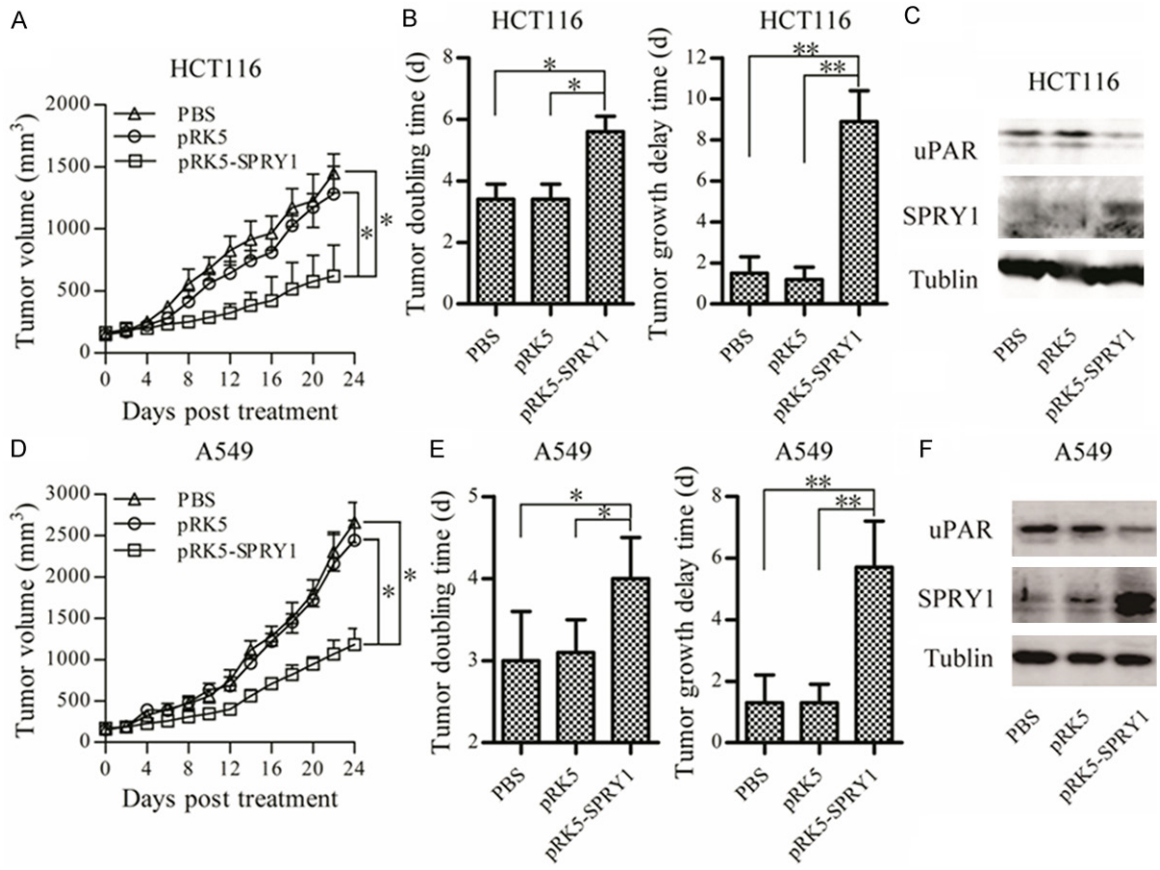

Figure 6. Delivery of SPRY1 to tumor tissues suppressed solid tumor growth. A549 or HCT116 cells were injected into 6-8-week-old BL/6mice. When tumors reached a size of 150 mm^3, mice were intratumorally injected with M-PEI complexed with SPRY1 overexpression vector or empty vector. Tumor volume comparison among different groups in nude mice bearing (A) HCT116 carcinomas and (D) A549 carcinomas (mean ± SD, n = 8, *P < 0.05, compared with each corresponding treatment). Tumor doubling time and tumor growth delay time comparison among different groups in nude mice bearing (B) HCT116 carcinomas and (E) A549 carcinomas. The results are expressed as mean ± SD from 8 animals. *P < 0.05, **P < 0.01 compared to control. SPRY1 and uPAR expression in HCT116 derived tumors (C) and A549 derived tumors (F) were determined by western blot analysis.

shown in **Figure 5A**, SPRY1 had minimal effects on proliferation of both cell lines at 24 h, whereas at 48 and 72 h, SPRY1 significantly inhibited both A549 and HCT116 cell growth.

Next, we tested if uPAR was involved in the proliferation pathway mediated by SPRY1. HCT116 wild-type cells (WT), uPAR downregulated stable cells (Antisense-uPAR) and controls (Mock) were transfected with SPRY1 overexpression vector or untransfected. Cells were reseeded 24 h later in RTCA 16-well plates and the proliferation was monitored by the RTCA system. As shown in **Figure 5B**, SPRY1 significantly inhibited the proliferation both of antisense-uPAR and mock cells compared with the vector control, which showed increased doubling times. We also found that SPRY1 has different degrees of maximal inhibition of proliferation in antisense-uPAR and mock cells. In mock cells, proliferation was inhibited by SPRY1 by 50%, but in antisense-uPAR cells, SPRY1 inhibited proliferation only by 30%.

Although other groups previously reported that SPRY1 reduces cell proliferation in vitro [29], the molecular mechanism underlying this process is still unclear. Most studies suggest that SPRY1 is an intrinsic inhibitor of the Ras/MEK/ERK pathway. Our results indicated an uPAR-mediated pathway that seems to be involved in the proliferation inhibitory effect of SPRY1. uPAR was reported to interact with transmembrane receptors, such as β1 integrin, which are frequently associated with the activation of the FAK-ERK pathway. Considering the above find-

ings, the activation of FAK and ERK in antisense-uPAR and mock cells transfected with SPRY1 or empty vector was evaluated. As shown in **Figure 5C**, antisense-uPAR cells transfected with SPRY1 over-expression vector result in FAK activation decreased by 19% and ERK activation decreased by 37% compared with empty vector transfection. While in mock cells, FAK and ERK activations were decreased by 38 and 59%, respectively. Considering the above results, we can conclude that SPRY1 inhibits proliferation via two distinct pathways: (1) as published by others, SPRY1 directly inhibits the growth factor receptor pathway as an intrinsic inhibitor of the Ras/MEK/ERK pathway, and (2) SPRY1 promotes degradation of uPAR, which leads inhibition of FAK/ERK activation.

For further validation of these results, HCT116 wide type cells were transiently transfected with uPAR alone or together with SPRY1 overexpression vector. Transfected cells were serum-starved overnight or not to eliminate the possibility that SPRY1 acts only as an inhibitor of growth factor signal transduction. As shown in **Figure 5D**, in the normal group (FBS+ group), SPRY1 overexpression alone inhibited the phosphorylation of ERK, uPAR overexpression alone significantly increased levels of phosphorylated ERK, and co-transfection of both inhibited increased ERK phosphorylation levels. Compared with the FBS+ group, overexpression of SPRY1 alone in the FBS- group had a slight effect on ERK activation, which was not significant. Overexpression of uPAR increased ERK activity, however, when uPAR was co-transfected with SPRY1, the uPAR-induced activation of ERK1/2 was inhibited. To further prove these observations, we used 293 cells, as these cells do not express endogenous uPAR. We expressed SPRY1 and uPAR together or alone in 293 cells and subsequently serum starved the cells overnight. SPRY1 alone did not suppress ERK activation, though SPRY1 co-transfected with uPAR blocked uPAR-induced activation of ERK1/2 (data not shown). Collectively, these data indicate that SPRY1 may *function* in cell proliferation pathways by inhibiting uPAR-induced activation of ERK.

Effect of SPRY1 on xenograft growth in a subcutaneous tumor model

The above results indicated that SPRY1 significantly inhibits proliferation of two low basal SPRY1 expression human cancer cell lines HCT116 and A549 *in vitro*. We next ascertained whether expression of SPRY1 also reduces the growth of these cells to form tumors *in vivo*. We injected A549 and HCT116 cells subcutaneously in athymic nude mice. When tumors reached a size of roughly 6.5 × 6.5 mm^2, we delivered SPRY1 overexpression plasmids to tumors using the transfection reagent GenEscort™, according to our previously reported method [30]. In brief, tumor-bearing mice were injected with transfection reagent complexed with SPRY1 overexpression plasmids or empty vector every 5 days for 15 days (three injections). After the first injection, tumor growth was measured every other day. As shown in **Figure 6A** and **6D**, treatment with SPRY1 overexpression plasmid greatly suppressed the growth of subcutaneous tumors produced by A549 or HCT116 cells. In mice bearing A549 xenografts, tumor doubling time was prolonged from 3.1 days (CI, 2.6–3.5 days) to 4.0 days (CI, 3.7–4.5 days) (**Figure 6B** and **Table 1**). In mice bearing HCT116 xenografts, tumor doubling time was prolonged from 3.4 days (CI, 3.1–3.9 days) to 5.6 days (CI, 5.3–6.1 days) (**Figure 6E** and **Table 1**). SPRY1 also caused a marked delay of 7.5 days (CI, 5.7–10.7 days) in mice bearing A549 xenografts and 11.7 days (CI, 3.8–13.7 days) in mice bearing HCT116 xenografts for tumor growth to 1000 mm^3 compared with PBS control (**Figure 6B**, **6E** and **Table 1**). We measured SPRY1 and uPAR protein levels in HCT116 cell– and A549 cell–derived tumors by Western blotting. As shows in **Figure 6C** and **6F**, overexpression of SPRY1 leads to decreased uPAR protein levels compared with PBS or empty vector treatment.

Discussion

uPAR is overexpressed in various aggressive cancer types and is closely associated with poor prognosis of cancers [31-33]. In recent years, several studies have revealed that uPAR is an essential factor for tumor cell invasion and metastasis. uPAR lacks transmembrane and intracellular domains and the mature uPAR is anchored to the cell surface through a GPI anchor. Several transmembrane co-receptors were reported to cooperate with uPAR to activate intracellular signaling. In addition, we and other groups have demonstrated that uPAR also interacts with some cytoplasmic proteins including SPRY1 [34-36]. However, the relation-

Table 1. Regression Analysis for Treatment Effects on Tumor Growth

	Treatment	Growth curves, V(t)[a]	r	Tumor doubling Time (d)[b]	Tumor growth delay (d)[c]
A549	PBS	Ln(V) = 0.235 d + 4.950	0.987	3.0 (2.8-3.6)	0 (0-1.2)
	pRK5	Ln(V) = 0.225 d + 4.995	0.977	3.1 (2.6-3.5)	1.3 (1.0-1.9)
	pRK5-SPRY1	Ln(V) = 0.174 d + 4.884	0.989	4.0 (3.7-4.5)*	7.5 (5.7-10.7)*
HCT116	PBS	Ln(V) = 0.207 d + 5.013	0.934	3.4 (3.1-3.9)	0 (0-1.5)
	pRK5	Ln(V) = 0.206 d + 4.863	0.971	3.4 (3.2-3.9)	1.5 (0.8-2.9)
	pRK5-SPRY1	Ln(V) = 0.124 d + 4.943	0.994	5.6 (5.3-6.1)*	11.7 (8.9-13.7)*

[a]Regression growth curves summarize volume (V, mm^3) dependence on time (d, days) from initial treatment, with correlation coefficients indicated by r. [b]Tumor doubling time was derived from exponential growth curves. [c]Growth delay was determined by assessing the time interval to 1000 mm^3. (Mean ± SD, *$p < 0.05$ compared with PBS).

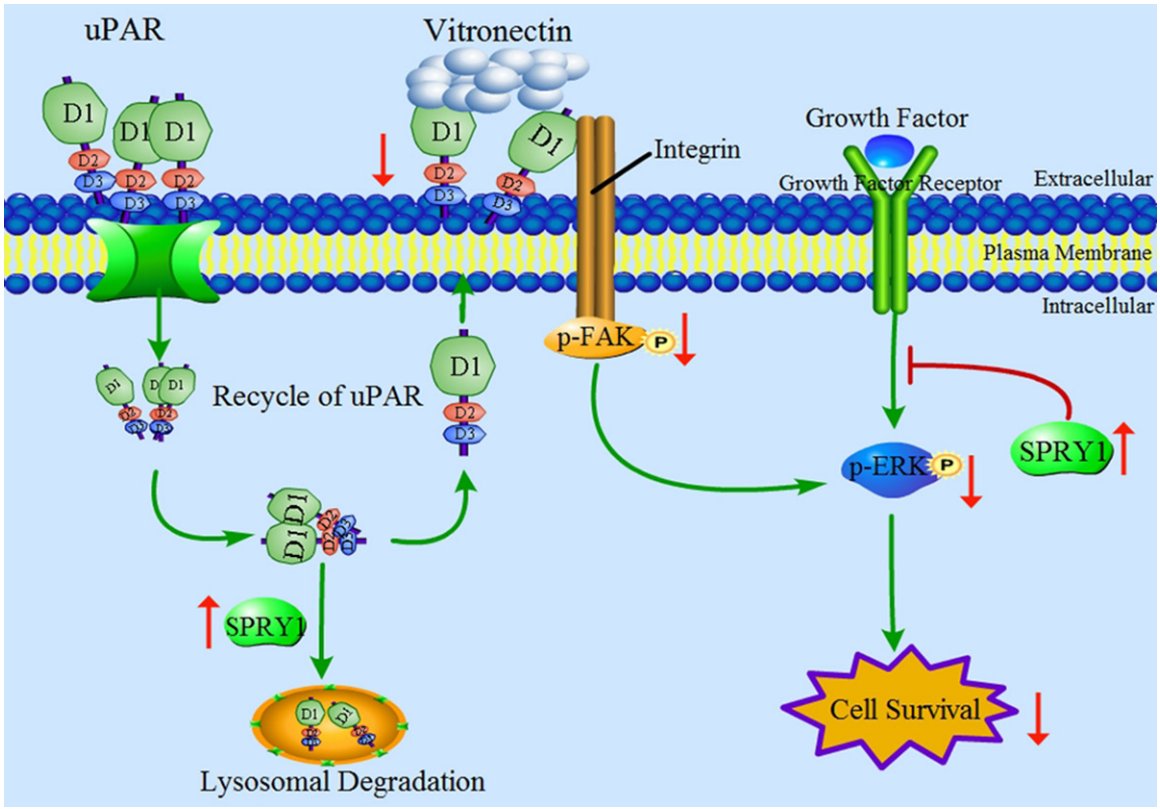

Figure 7. Schematic model of the proposed mechanism for SPRY1 promotion of lysosomal degradation of uPAR and inhibition of uPAR-mediated cell adhesion and proliferation. First, upregulation of SPRY1 could inhibit growth factor receptor signaling pathway and inhibit Raf/MEK/ERK-induced proliferation. On the other hand, SPRY1 interacts with uPAR to trigger degradation of uPAR via the lysosomal pathway, and then decrease the amount of uPAR recycled back to the cell surface. Cell surface uPAR decrease not only reduces adhesion functions, but also inhibits activation of FAK and ERK, which finally inhibits cell proliferation.

ship of these interactions with cellular functions remains unclear. Here, we report that SPRY1 interacts with uPAR and promotes its degradation via the lysosomal pathway. SPRY1 also inhibits uPAR-dependent adhesion to vitronectin as well as augments cell proliferation both *in vitro* and *in vivo*.

Cell surface uPAR can be internalized and recycled to the leading edge. This process is considered to have an important role in regulating the level and distribution of cell surface uPAR, thus controlling uPAR proteolysis functions [37]. How uPAR is internalized into the cytoplasm and whether it is degraded has not been completely established. At least two different mechanisms have been proposed. First, in ligand-induced internalization, uPAR can be internalized through its interaction with uPA/PAI-1 complexes, and uPA and PAI-1 are eventually

degraded in the lysosome while uPAR could be recycled back to the plasma membrane [38]. Alternatively, uPAR can also be efficiently internalized by ENDO180, an uPAR-associated protein. ENDO180 promotes uPAR internalization and transports uPAR to lysosomal compartments for degradation [39]. Second, in a ligand-independent internalization pathway, uPAR can be constitutively internalized in an uPA/PAI-1- and lipid raft-independent manner and this is associated with rapid recycling of uPAR to the cell surface, during which uPAR does not reach lysosomes [10]. Since the recycling of uPAR is rapid, internalized uPAR direct recycling to the plasma membrane or trafficking to the lysosome or proteasome for degradation may be important for the regulation of cell function. Our current results add another dimension to intercellular uPAR degradation and provide evidence that SPRY1 promotes uPAR degradation through the lysosomal pathway.

In mammals, four SPRY genes (SPRY1–4) have been found. All SPRY isoforms possess a highly conserved N-terminal tyrosine residue. SPRY1 is a candidate tumor suppressor gene and its expression is deregulated in several cancer types such as medullary thyroid carcinoma [29], breast [21], prostate [22] and liver cancers [23]. More recently, a study revealed SPRY1, as a direct target of miR-21, regulates several pathologic processes, including cancer [26], atrial fibrillation (AF) [40], and vascular and metabolic disease [41]. To date, the function of SPRY1 in cancer development has been believed to act as a negative feedback inhibitor of RTK signaling. Meanwhile, other studies have also found that SPRY1 can induce cellular senescence [42]. Our current results expand SPRY1 function and provide evidence that SPRY1 can also regulate uPAR stability independently of its ability to regulate the RTK signaling. SPRY proteins can interact with multiple components of the Ras/MAPK pathway, but other interacting molecules are largely unknown. We showed co-localization between uPAR and SPRY1 in the cytoplasm (**Figure 2**). Furthermore, we revealed that SPRY1 interacts with uPAR and promotes its degradation through the lysosome pathway. Forced expression of SPRY1 increased the degradation of uPAR proteins (**Figure 3**). A previous study indicated that SPRY1 associates with Caveolin-1, the major structural protein of caveolae [43], which may be in functional agreement with a previous study in which uPAR was also reported to interact with Caveolin-1 [44]. Thus, we speculate that uPAR, Caveolin-1 and SPRY1 may form a tripartite complex. However, this hypothesis and the cellular implications of this interaction will require further investigation.

We also showed here that SPRY1 overexpression augments uPAR induced cell adhesion and proliferation. Vitronectin binding to uPAR is an important event in wound healing, tissue remodeling, immune response, and cancer. Previous studies have shown that uPAR can mediate cell adhesion to vitronectin [2]. The exact mechanism of how SPRY1 regulates uPAR to decrease adhesion to vitronectin is unclear. Our results indicated that this may be, at least in part, caused by the reduced amounts of cell surface uPAR (**Figure 4C**). Our preliminary data revealed extremely low basal expression of SPRY1 in HCT116 human colon carcinoma cells and A549 lung carcinoma cell lines (**Figure 1**). Forced expression of SPRY1 in HCT116 cells inhibited proliferation of cells. Meanwhile, FAK and ERK phosphorylation was decreased.

Sustained ERK1/2 activity is strongly associated with many types of cancers, such as prostate, colon and lung cancer [45]. Previous data showed that activation of ERK by uPAR may primarily promote cell proliferation [46]. Additionally, increasing evidence showed that down-regulation of uPAR resulted in greatly decreased activity of the ERK signaling pathway [47, 48]. Our results showed that SPRY1 inhibited the proliferation of cancer cells both in vivo and in vitro (**Figures 5** and **6**). We overexpressed uPAR and SPRY1 alone or together in HCT116 cells, and found that overexpression of SPRY1 decreased ERK1/2 phosphorylation and that this effect was higher in uPAR co-expressed conditions (**Figure 5D**). To test whether the inhibited proliferation was related to uPAR or only because of SPRY1 inhibition of RTK signaling, we repeated the same experiment in 293T cell lines, which lack endogenous uPAR. Similar to the results obtained in HCT116 cells, upregulation of SPRY1 decreased uPAR-induced ERK activation, but SPRY1 alone did not affect ERK phosphorylation. These results collectively indicate that increasing the expression of SPRY1 in cells may be beneficial not only for inhibiting MAPK activation induced by several growth factor stimuli, but also for decreasing uPAR-induced sustained ERK activation.

In conclusion, our results show that in addition to functioning as an inhibitor of RTK signaling, SPRY1 can regulate crucial processes induced by uPAR (**Figure 7**). These results may open new perspectives for cancer biotherapy.

Acknowledgements

The authors are grateful to grants from the Ministry of Science and Technology (2012CB967004, 2014CB744501, 2012AA020304), the Chinese National Natural Sciences Foundation (81121062, 31200572), the Jiangsu Provincial Nature Science Foundation (BE2013630 and BZ2012050), the Bureau of Science and Technology of Changzhou, Jiangsu, China (CZ20130011, CE20135013, CZ20120004, CM20122003 and WF201207).

Disclosure of conflict of interest

The authors indicated no potential conflicts of interest.

Address correspondence to: Zi-Chun Hua, The State Key Laboratory of Pharmaceutical Biotechnology, College of Life Science, Nanjing University, 22 Han Kou Road Nanjing 210093, China. Tel: +86-25-83324605; Fax: +86-25-83324605; E-mail: zchua@nju.edu.cn; Yao Wang, Division of Critical Care and Surgery, St. George Hospital, University of New South Wales, Sydney, NSW 2217, Australia. Tel: +61-2-95293680; Fax: +61-2-95293680; E-mail: yao_wang_au@yahoo.com

References

[1] Alpízar-Alpízar W, Nielsen BS, Sierra R, Illemann M, Ramírez JA, Arias A, Durán S, Skarstein A, Ovrebo K, Lund LR, Laerum OD. Urokinase plasminogen activator receptor is expressed in invasive cells in gastric carcinomas from high- and low-risk countries. Int J Cancer 2010; 126: 405-15.

[2] Wei Y, Waltz DA, Rao N, Drummond RJ, Rosenberg S, Chapman HA. Identification of the urokinase receptor as an adhesion receptor for vitronectin. J Biol Chem 1994; 269: 32380-8.

[3] Bohuslav J, Horejsí V, Hansmann C, Stöckl J, Weidle UH, Majdic O, Bartke I, Knapp W, Stockinger H. Urokinase plasminogen activator receptor, beta 2-integrins, and Src-kinases within a single receptor complex of human monocytes. J Exp Med 1995; 181: 1381-90.

[4] Resnati M, Guttinger M, Valcamonica S, Sidenius N, Blasi F, Fazioli F. Proteolytic cleavage of the urokinase receptor substitutes for the agonist-induced chemotactic effect. EMBO J 1996; 15: 1572-82.

[5] Nalla AK, Asuthkar S, Bhoopathi P, Gujrati M, Dinh DH, Rao JS. Suppression of uPAR retards radiation-induced invasion and migration mediated by integrin β1/FAK signaling in medulloblastoma. PLoS One 2010; 5: e13006.

[6] Gondi CS, Kandhukuri N, Dinh DH, Gujrati M, Rao JS. Down-regulation of uPAR and uPA activates caspase-mediated apoptosis and inhibits the PI3K/AKT pathway. Int J Oncol 2007; 31: 19-27.

[7] Goretzki L, Mueller BM. Low-density-lipoprotein-receptor-related protein (LRP) interacts with a GTP-binding protein. J Cell Sci 1997; 110: 1395-402.

[8] Sturge J, Wienke D, East L, Jones GE, Isacke CM. GPI-anchored uPAR requires Endo180 for rapid directional sensing during chemotaxis. J Cell Biol 2003; 162: 789-94.

[9] Vilhardt F, Nielsen M, Sandvig K, van Deurs B. Urokinase-type plasminogen activator receptor is internalized by different mechanisms in polarized and nonpolarized Madin-Darby canine kidney epithelial cells. Mol Biol Cell 1999; 10: 179-95.

[10] Cortese K, Sahores M, Madsen CD, Tacchetti C, Blasi F. Clathrin and LRP-1-independent constitutive endocytosis and recycling of uPAR. PLoS One 2008; 3: e3730.

[11] Langkilde A, Hansen TW, Ladelund S, Linneberg A, Andersen O, Haugaard SB, Jeppesen J, Eugen-Olsen J. Increased plasma soluble uPAR level is a risk marker of respiratory cancer in initially cancer-free individuals. Cancer Epidemiol Biomarkers Prev 2011; 20: 609-18.

[12] Edsfeldt A, Nitulescu M, Grufman H, Grönberg C, Persson A, Nilsson M, Persson M, Björkbacka H, Gonçalves I. Soluble urokinase plasminogen activator receptor is associated with inflammation in the vulnerable human atherosclerotic plaque. Stroke 2012; 43: 3305-12.

[13] Wei C, E Hindi S, Li J, Fornoni A, Goes N, Sageshima J, Maiguel D, Karumanchi SA, Yap HK, Saleem M, Zhang Q, Nikolic B, Chaudhuri A, Daftarian P, Salido E, Torres A, Salifu M, Sarwal MM, Schaefer F, Morath C, Schwenger V, Zeier M, Gupta V, Roth D, Rastaldi MP, Burke G, Ruiz P, Reiser J. Circulating urokinase receptor as a cause of focal segmental glomerulosclerosis Nat Med 2011; 17: 952-60.

[14] Berres ML, Schlosser B, Berg T, Trautwein C, Wasmuth HE. Soluble urokinase plasminogen activator receptor is associated with progressive liver fibrosis in hepatitis C infection. J Clin Gastroenterol 2012; 46: 334-8.

[15] Edwin F, Anderson K, Ying C, Patel TB. Intermolecular interactions of Sprouty proteins and

their implications in development and disease. Mol Pharmacol 2009; 76: 679-91.
[16] Hanafusa H, Torii S, Yasunaga T, Nishida E. Sprouty1 and Sprouty2 provide a control mechanism for the Ras/MAPK signalling pathway. Nat Cell Biol 2002; 4: 850-8.
[17] Tefft D, Lee M, Smith S, Crowe DL, Bellusci S, Warburton D. mSprouty2 inhibits FGF-activated MAP kinase by differentially binding to upstream target proteins. Am J Physiol Lung Cell Mol Physiol 2002; 283: L700-6.
[18] Wong ES, Lim J, Low BC, Chen Q, Guy GR. Evidence for direct interaction between Sprouty and Cbl. J Biol Chem 2001; 276: 5866-75.
[19] Fong CW, Leong HF, Wong ES, Lim J, Yusoff P, Guy GR. Tyrosine phosphorylation of Sprouty2 enhances its interaction with c-Cbl and is crucial for its function. J Biol Chem 2003; 278: 33456-64.
[20] Sasaki A, Taketomi T, Kato R, Saeki K, Nonami A, Sasaki M, Kuriyama M, Saito N, Shibuya M, Yoshimura A. Mammalian Sprouty4 suppresses Ras-independent ERK activation by binding to Raf1. Nat Cell Biol 2003; 5: 427-32.
[21] Lo TL, Yusoff P, Fong CW, Guo K, McCaw BJ, Phillips WA, Yang H, Wong ES, Leong HF, Zeng Q, Putti TC, Guy GR. The ras/mitogen-activated protein kinase pathway inhibitor and likely tumor suppressor proteins, sprouty 1 and sprouty 2 are deregulated in breast cancer. Cancer Res 2004; 64: 6127-36.
[22] Kwabi-Addo B, Wang J, Erdem H, Vaid A, Castro P, Ayala G, Ittmann M. The expression of Sprouty1, an inhibitor of fibroblast growth factor signal transduction, is decreased in human prostate cancer. Cancer Res 2004; 64: 4728-35.
[23] Fong CW, Chua MS, McKie AB, Ling SH, Mason V, Li R, Yusoff P, Lo TL, Leung HY, So SK, Guy GR. Sprouty 2, an inhibitor of mitogen-activated protein kinase signaling, is down-regulated in hepatocellular carcinoma. Cancer Res 2006; 66: 2048-58.
[24] Gross I, Morrison DJ, Hyink DP, Georgas K, English MA, Mericskay M, Hosono S, Sassoon D, Wilson PD, Little M, Licht JD. The receptor tyrosine kinase regulator Sprouty 1 is a target of the tumor suppressor WT1 and important for kidney development. J Biol Chem 2003; 278: 41420-30.
[25] Sabatel C, Cornet AM, Tabruyn SP, Malvaux L, Castermans K, Martial JA, Struman I. Sprouty1, a new target of the angiostatic agent 16K prolactin, negatively regulates angiogenesis. Mol Cancer 2010; 9: 231.
[26] Jin XL, Sun QS, Liu F, Yang HW, Liu M, Liu HX, Xu W, Jiang YY. microRNA 21-mediated suppression of Sprouty1 by Pokemon affects liver cancer cell growth and proliferation. J Cell Biochem 2013; 114: 1625-33.
[27] Ranson M, Andronicos NM, O'Mullane MJ, Baker MS. Increased plasminogen binding is associated with metastatic breast cancer cells: differential expression of plasminogen binding proteins. Br J Cancer 1998; 77: 1586-97.
[28] Mekkawy AH, De Bock CE, Lin Z, Morris DL, Wang Y, Pourgholami MH. Novel protein interactors of urokinase-type plasminogen activator receptor. Biochem Biophys Res Commun 2010; 399: 738-43.
[29] Macià A, Gallel P, Vaquero M, Gou-Fabregas M, Santacana M, Maliszewska A, Robledo M, Gardiner JR, Basson MA, Matias-Guiu X, Encinas M. Sprouty 1 is a candidate tumor-suppressor gene in medullary thyroid carcinoma. Oncogene 2012; 31: 3961-72.
[30] Zhuang H, Jiang W, Zhang X, Qiu F, Gan Z, Cheng W, Zhang J, Guan S, Tang B, Huang Q, Wu X, Huang X, Jiang W, Hu Q, Lu M, Hua ZC. Suppression of HSP70 expression sensitizes NSCLC cell lines to TRAIL-induced apoptosis by upregulating DR4 and DR5 and downregulating c-FLIP-L expressions. J Mol Med 2013; 91: 219-35.
[31] Duffy MJ. The urokinase plasminogen activator system: role in malignancy. Curr Pharm Des 2004; 10: 39-49.
[32] Kita Y, Fukagawa T, Mimori K, Kosaka Y, Ishikawa K, Aikou T, Natsugoe S, Sasako M, Mori M. Expression of uPAR mRNA in peripheral blood is a favourite marker for metastasis in gastric cancer cases. Br J Cancer 2009; 100: 153-9.
[33] Giannopoulou I, Mylona E, Kapranou A, Mavrommatis J, Markaki S, Zoumbouli Ch, Keramopoulos A, Nakopoulou L. The prognostic value of the topographic distribution of uPAR expression in invasive breast carcinomas. Cancer Lett 2007; 246: 262-7.
[34] Kriegbaum MC, Persson M, Haldager L, Alpízar-Alpízar W, Jacobsen B, Gårdsvoll H, Kjær A, Ploug M. Rational targeting of the urokinase receptor (uPAR): development of antagonists and non-invasive imaging probes. Curr Drug Targets 2011; 12: 1711-28.
[35] De Bock CE, Lin Z, Mekkawy AH, Byrne JA, Wang Y. Interaction between urokinase receptor and heat shock protein MRJ enhances cell adhesion. Int J Oncol 2010; 36: 1155-63.
[36] Mekkawy AH, Morris DL, Pourgholami MH. HAX1 augments cell proliferation, migration, adhesion, and invasion induced by Urokinase-Type Plasminogen Activator Receptor. J Oncol 2012; 2012: 950749.
[37] Webb DJ, Nguyen DH, Gonias SL. Extracellular signal-regulated kinase functions in the urokinase receptor-dependent pathway by which neutralization of low density lipoprotein receptor-related protein promotes fibrosarcoma cell migration and matrigel invasion. J Cell Sci 2000; 113: 123-34.

[38] Conese M, Blasi F. Urokinase/urokinase receptor system: internalization/degradation of urokinase-serpin complexes, mechanism and regulation. Biol Chem Hoppe Seyler 1995; 376: 143-55.
[39] Kjøller L, Engelholm LH, Høyer-Hansen M, Danø K, Bugge TH, Behrendt N. uPARAP/endo180 directs lysosomal delivery and degradation of collagen IV. Exp Cell Res 2004; 293: 106-16.
[40] Cardin S, Guasch E, Luo X, Naud P, Le Quang K, Shi Y, Tardif JC, Comtois P, Nattel S. Role for MicroRNA-21 in atrial profibrillatory fibrotic remodeling associated with experimental postinfarction heart failure. Circ Arrhythm Electrophysiol 2012; 5: 1027-35.
[41] Cheng Y, Zhang C. MicroRNA-21 in cardiovascular disease. J Cardiovasc Transl Res 2010; 3: 251-5.
[42] Macià A, Vaquero M, Gou-Fàbregas M, Castelblanco E, Valdivielso JM, Anerillas C, Mauricio D, Matias-Guiu X, Ribera J, Encinas M. Sprouty1 induces a senescence-associated secretory phenotype by regulating NFκB activity: implications for tumorigenesis. Cell Death Differ 2014; 21: 333-43.
[43] Cabrita MA, Jäggi F, Widjaja SP, Christofori G. A functional interaction between sprouty proteins and caveolin-1. J Biol Chem 2006; 281: 29201-12.
[44] Wei Y, Yang X, Liu Q, Wilkins JA, Chapman HA. A role for caveolin and the urokinase receptor in integrin-mediated adhesion and signaling. J Cell Biol 1999; 144: 1285-94.
[45] Hoshino R, Kohno M. Constitutive activation of the ERK-MAP kinase pathway in human tumors. Seikagaku 2000; 72: 460-5.
[46] Aguirre-Ghiso JA, Liu D, Mignatti A, Kovalski K, Ossowski L. Urokinase receptor and fibronectin regulate the ERK (MAPK) to p38 (MAPK) activity ratios that determine carcinoma cell proliferation or dormancy in vivo. Mol Biol Cell 2001; 12: 863-879.
[47] Nowicki TS, Zhao H, Darzynkiewicz Z, Moscatello A, Shin E, Schantz S, Tiwari RK, Geliebter J. Downregulation of uPAR inhibits migration, invasion, proliferation, FAK/PI3K/Akt signaling and induces senescence in papillary thyroid carcinoma cells. Cell Cycle 2011; 10: 100-7.
[48] Xue A, Xue M, Jackson C, Smith RC. Suppression of urokinase plasminogen activator receptor inhibits proliferation and migration of pancreatic adenocarcinoma cells via regulation of ERK/p38 signaling. Int J Biochem Cell Biol 2009; 41: 1731-8.